2nd Australian Microwave Symposium, Adelaide, Australia, 11 - 12 February 2016

Experimental and Numerical Analysis of Nonlinear Left Handed Transmission Lines using Three Wave Mixing

Sameh Y. Elnaggar and Gregory N. Milford
School of Engineering & Information Technology, University of New South Wales
ADFA, Northcott Drive, Canberra, 2600 Australia
g.milford@adfa.edu.au

***Abstract*—In this paper, we demonstrate the use of three wave mixing and quasi phase matching to describe the parametric behaviour of a Nonlinear Composite Right-Left Handed Transmission Line. The varactor's configuration plays an essential role in determining the parametric frequencies. The findings are verified using simulation and measurement.**

Keywords: nonlinear left-handed transmission line, phase matching, three wave mixing, parametric generation.

I. Introduction

The intriguing properties of Left-handed or Composite Right-Left handed transmission lines (CRLH TL) were successfully exploited to realize novel microwave devices [1], [2]. Nonlinear behaviour can be stimulated by incorporating nonlinear reactive components (varactor diodes, for example). It was demonstrated that nonlinear (NL) CRLH TLs can have interesting phenomena such as harmonic, subharmonic and parametric generation, envelope solitons and multistabilty [3].

The study of the parametric and harmonic generation of NL CRLH TL has gained recent interest. Nonlinear optics-like approaches were applied to NL CRLH TL structures [4], [3]. In the following we demonstrate how parametric components generated by the application of a strong pump can be explained using three-wave mixing and Quasi Phase Matching. The similarity and differences between our approach and the approaches used in nonlinear optics are noted.

II. TL analysis

A NL CRLH TL can be realized by incorporating series varactors within a host microstrip structure. Fig. 1 shows the lumped element equivalent circuit of two unit cells of such a structure. Left-handed behaviour results from shunt inductance L_L and series capacitance C_L (ie. series varactors) with L_R and C_R modeling the right-handed microstrip TLs. In Fig. 1 the two varactors are shown mounted back to back. This is a practical and convenient configuration to reverse bias the varactors. The varactor capacitance C_L and hence the charge stored in the varactors are nonlinear functions of the terminal voltages U_n.

The polarity of the accumulated charge on C_L depends on the varactor position in the circuit. For example, the charge on the left 'plate' (diffusion region) of the n^{th} capacitor is negative, since the first encountered region is the P type, which

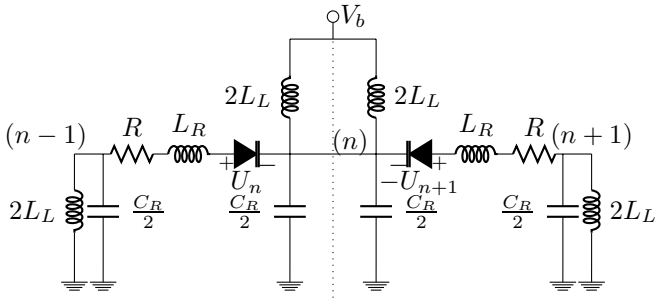

Fig. 1. (The lumped cricuit model of two unit cells. The n$^{\text{th}}$ varactor's equivalent capacitance C_L is a function of the voltage U_n. Typical values: $L_L = 1.797$ nH, $C_R = 1.1$ pF, $L_R = 2.7$ nH, $C_L = 0.73$ pF, with $C_1 = 0.22$ pF/V for a balanced configuration (no band gap) [5].

is predominately full of acceptor ions. On the contrary, the N type region is first encountered for the $(n+1)^{\text{th}}$ diode and hence the charge polarity is positive. Taking this into account, the charge Q_n stored in the n^{th} varactor can be expressed in terms of the terminal voltage U_n. Expanding the charge as a Taylor series around the bias voltage produces:

$$Q_n = (-1)^n |Q_n|_{V_B} + C_L|_{V_B} \left[U_n - (-1)^n V_B\right] - (-1)^n \frac{C_1|_{V_B}}{2} \left[U_n - (-1)^n V_B\right]^2 \quad (1)$$

In (1) we assume that the varactor charge dependance can be described by a quadratic nonlinearity, with coefficient C_1. It is worth mentioning that because the nonlinearity is due to the series capacitance, it is of magnetic type. Moreover, the nonlinearity is equivalent to the nonlinear susceptibility in nonlinear optical materials. The sign alternation in (1) is a consequence of the varactor orientations, and is similar to *periodic polling* in optics, where birefringent dielectric layers are periodically oriented to compensate for the mismatch between a pump and its parametric components. This technique is known as Quasi Phase Matching (QPM). However, there is a subtle but rather crucial difference between NL CRLH TLs and nonlinear optical materials. Unlike effective media parameters, the nonlinearity introduced here is microscopic (sub-wavelength) in nature.

By limiting the interaction to be between an input pump excitation and two induced parametric components, a three wave

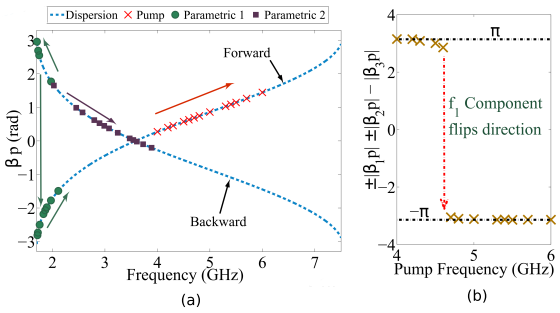

Fig. 2. (a) The simulated parametric components values plotted on the $f, \beta p$ curves for forward and backward travelling waves. The arrows indicate the trajectories of the different components as the pump frequency increases. (b) The calculated QPM condition using (2) and (3).

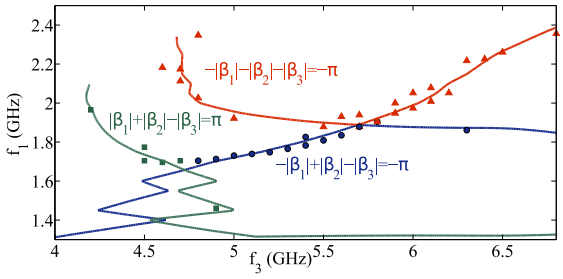

Fig. 3. The measured QPM conditions plotted against the expected measured QPM conditions based on (2) to (4).

mixing approach can be used. For efficient parametric generation the parametric components should be phase matched with the pump. The alternation of the sign of the quadratic nonlinearies, along with no constraint on propagation direction (forward or backward) for the parametric components, results in the following phase matching conditions:

$$+|\beta_1 p| + |\beta_2 p| - |\beta_3 p| = +\pi \quad (2)$$

$$-|\beta_1 p| + |\beta_2 p| - |\beta_3 p| = -\pi \quad (3)$$

$$-|\beta_1 p| - |\beta_2 p| - |\beta_3 p| = -\pi \quad (4)$$

$$f_1 + f_2 = f_3 \quad (5)$$

where $\beta_1 p$, $\beta_2 p$ and $\beta_3 p$ are the phase shift per unit cell, at frequencies f_1, f_2 and f_3, of the first, second parametric and pump components, respectively, (signs of $\beta_x p$ referenced to forward travelling waves), and p is the unit cell length.

III. Results and Discussion

A. Numerical Analysis

Simulation of a relatively long TL of 80 sections is achieved using state space modelling [6]. Using a long TL guarantees that reflections from the source and load ports are minimized. Fig. 2(a) shows the loci of the pump and parametric components depicted on the calculated dispersion relation $(f, \beta p)$ for forward and backward travelling waves, obtained using the ABCD parameters [2] for the unit cell of Fig. 1, while Fig. 2(b) shows the dependence of the QPM conditions on pump frequency. As the forward travelling right handed pump frequency increases, positive valued $\beta_3 p$ increases (crosses in Fig. 2). From (5), the net sum of f_1 and f_2 increases. The only possibility is that indicated by the circles in the upper left in Fig. 2, corresponding to a backward travelling, left handed parametric component with frequency f_1 decreasing as it moves toward the lower Bragg frequency, hence $|\beta_1 p|$ increases towards π. At the same time the f_2 parametric component increases in frequency to compensate for the pump frequency increase, resulting in a backward travelling, left handed f_2 component where $|\beta_2 p|$ decreases towards zero such that (2) is satisfied. As f_3 increases further, f_1 will reach the Bragg frequency, where the phase shift is $\pm\pi$. Any further increase in f_3 produces a flip in the propagation direction of the f_1 component, indicated by the circles in the lower left of Fig. 2(a), corresponding to a forward travelling f_1 component, with the still backward travelling f_2 component, now satisfying (3).

B. Measurements

Measurement of the parametric frequencies was carried out on a 20-stage NL CRLH TL [5]. In this case, a pump signal was applied using a signal generator. The output port was connected to a specturm analyzer. For each pump frequency f_3, the pump power was increased until the parametric components started to emerge from the noise floor. Using the extracted dispersion relation [5], the corresponding $\beta_1 p$, $\beta_2 p$ and $\beta_3 p$ were determined. The different combinations in (2) to (4) were calculated for each parametric pair. An algorithm was developed to bookkeep the parametric pairs which satisfy one of the conditions within an 8% tolerance to take into account errors due to the short length of the TL, uncertainties in the extracted dispersion and measurement errors.

In addition, the frequencies f_1 and f_2 that satisfy the conditions (2) to (5) were determined for a range of f_3 values, resulting in the solid curves in Fig. 3. These curves define the frequencies at which (2) to (4) are satisfied. The measured phase matching conditions are also depicted in Fig. 3. It is clear that the measured parametric components *do* satisfy (2) to (5). The three-wave mixing and QPM provide a promising framework to engineer the dispersion relation for efficient and predictable parametric generation.

References

[1] G. V. Eleftheriades and K. G. Balmain, *Negative-Refraction Metamaterials Fundamental Principles and Applications*. Wiley, 2005.

[2] C. Caloz and T. Itoh, *Electromagnetic Metamaterials Transmission Line Theory and Microwave Applications*. Wiley, 2006.

[3] A. B. Kozyrev and D. W. van der Weide, "Nonlinear left-handed transmission line metamaterials," *Journal of Physics D: Applied Physics*, vol. 41, no. 17, p. 173001, 2008.

[4] R. W. Boyd, *Nonlinear optics*, 3rd ed. Boston: Boston : Academic Press, 2008.

[5] G. Milford and M. Gibbons, "Parametric frequency radiation from a nonlinear CRLH transmission line," in *Microwave Conference Proceedings (APMC), 2011 Asia-Pacific*, Dec 2011, pp. 538–541.

[6] S. Y. Elnaggar and G. N. Milford, "Analysis of nonlinear Left-Handed transmission lines using state space modelling," in *2015 International Symposium on Antennas and Propagation (ISAP) (ISAP2015)*, Hobart, Australia, Nov. 2015.